Sensors and Materials, Vol. 9, No. 5 (1997) 279–296
MYU Tokyo

S & M 0292

The Stability of Tin and Indium Oxide Thin Film Gas Sensors

Constantinos A. Papadopoulos, Demetrios S. Vlachos and John N. Avaritsiotis

National Technical University of Athens
Department of Electrical and Computer Engineering, Division of Computer Science
9 Heroon Polytechniou St., 157 73 Zographou, Athens, Greece

(Received April 2, 1996; accepted November 5, 1996)

Key words: metal oxide thin film gas sensors, noble metal additives, sensor degradation, sensor selectivity, gas classification

Tin and indium oxide reactively sputtered thin films, surface doped with palladium and platinum, are evaluated as sensors for carbon monoxide, methane, propane, n-butane and ethanol. The sensors are subjected to continuous heating to 450°C – cooling to 150°C cycles, in order to determine their degradation with continuous use. A simple nonparametric technique is used in order to determine the stability, interdependence and selectivity of the sensors. Useful results are obtained concerning the stability of sensors with different sensing layers and different catalysts deposited onto their surfaces. Sensors with different thicknesses of the same additive are found to be strongly correlated (i.e., they exhibit similar responses to the same test gases at the same temperatures; this is often referred to as collinearity in the sense that the response vector of one sensor can be derived from the response vector of another sensor by simply multiplying with a constant), while those with different additives are found to be uncorrelated. Finally, platinum-doped sensors were found to be selective, i.e., to exhibit different responses in the presence of different gases, while undoped or palladium-doped ones were found to be nonselective. Such results derived from simple techniques can be used to evaluate sensors incorporated in a multisensor pattern recognition array.

1. Introduction

The discovery that existing metal oxide gas sensing materials have poor selectivity has given impetus to a design philosophy that utilizes arrays of sensors within multisensor systems.[1,2] In order to develop reliable systems which do not require frequent calibration,

the response of the sensors used must remain stable during continuous use. The resistance of oxygen-deficient metal oxides exhibits a continuous drift with use, due to the high temperatures required for their operation, leading to a continuous degradation which is attributed to surface reduction of the oxides.[3] Consequently, a system based on resistive-type gas sensors requires recalibration after a relatively short period of time.

In this study we considered reactively sputtered tin oxide (SnO_x) and indium oxide (InO_x) thin films as potential elements of sensor arrays for five gases, namely carbon monoxide, methane, propane, n-butane and ethanol. Thin film resistive-type sensors which exhibit different responses to the aforementioned gases were fabricated. For this purpose pappadium and platinum noble metals were deposited on the surface of the films. The responses of the sensors were considered as vectors. Selectivity and interdependence could be quantified and expressed with a number, if we calculate correlation coefficients using the appropriate response vectors. In addition, the sensors were subjected to successive thermal cycles and the correlation coefficients relating to the responses of the same sensor before and after a predetermined number of thermal cycles were thought to provide a measure of stability.

2. Materials and Methods

Deposition of SnO_x and InO_x films was performed using a Leybold Z-400 planar magnetron sputtering system, which was d. c. operated in a controlled, high-purity Ar-O_2 mixture. Two different discharge modes were obtained, the metallic mode and the reactive mode, where the target was respectively free from or covered with reaction products. The reactions for compound formation were desirable in the metallic mode for high-rate depositions, and for more precise control of the O_2/metal (Sn or In) ratio in the deposited film. This necessitated the use of a plasma emission monitor (PEM) system that allowed us to select and maintain the degree of target oxidation,[4] with the tin or indium emission line intensity at 450 nm as a measurement for the control loop of the reactive gas mass flow controller. This technique was proven adequate for the fabrication of reproducible films.

Sputtering was performed on Al_2O_3 (96%) substrates with an area of 12 × 26 mm, heated to 300°C. Films were fabricated at a relatively high total gas pressure of approximately 1.0×10^{-2} mbar. The substrate holder was positioned at a distance of 70 mm from the 100-mm-diameter target. The total power introduced into the tin or indium target was 115 W with a total current of 0.36 A, thus achieving a deposition rate of approximately 100 nm/min. Argon flow was adjusted manually to 20 ml/min, while oxygen intake was controlled by the aforementioned PEM control unit, so that the intensity of the metal (tin or indium) emission line remained constant. An O_2 flow of around 30 ml/min was found to give an appropriate O_2/metal (tin or indium) ratio, so that the fabricated films could function as sensors with a base resistance below 30 MΩ at 100°C in the presence of zero grade air at ambient pressure (a low oxygen to metal ratio gives metallic films and a high oxygen to metal ratio gives highly resistive films). The thickness of all the fabricated films was equal to 1000 nm (10 min sputtering time). Films were not annealed. The eight tin oxide films and the eight indium oxide films, which were fabricated under identical

conditions, showed electrical properties within a 10% tolerance.

Palladium was subsequently electron-beam-evaporated on three of the aforementioned tin oxide (SnO_x) films and on four of the aforementioned indium oxide (InO_x) films. Platinum was deposited on the four SnO_x films and on the other four InO_x films. One tin oxide film was left undoped (without additive). Evaporation was performed using an Edwards 306 vacuum evaporation apparatus. Total pressure during electron beam evaporation was about 3×10^{-5} mbar (the evaporation chamber was evacuated from ambient air) and the substrates were not heated during evaporation. Evaporation was carried out at relatively low deposition rates of the order of 0.3 nm/s for palladium and 0.1 nm/s for platinum. Palladium was deposited on three tin oxide (SnO_x) and three indium oxide (InO_x) films with evaporation times of 5, 10 and 20 s. On the fourth InO_x film, the palladium deposition time was 30 s. Thus three SnO_x and four InO_x films, with an increasing palladium layer thickness on each of them, were fabricated. We refer to these sensors as SnO_x + Pd1, SnO_x + Pd2, SnO_x + Pd3, InO_x + Pd1, InO_x + Pd2, InO_x + Pd3 and InO_x + Pd4, depending on palladium layer thickness. Platinum was deposited on four tin oxide (SnO_x) and four indium oxide (InO_x) films in the same manner but at a much lower rate (0.1 nm/s) with evaporation times of 10, 20, 30 and 40 s. In an analogous sense we refer to these sensors as SnO_x + Pt1, ..., InO_x + Pt4. The average thickness of the metal films deposited onto the oxide surfaces was evaluated by activation energy measurements, using the procedure described in the literature,[5] and was found to be around 3–5 nm.

The sensor characterization setup was designed to measure the steady-state and transient response of the samples, testing them at various working temperatures and under different gas compositions. The testing conditions were rigorously controlled via a fully automated, computer controlled system. All sensors were characterized according to the following experimental procedure.

- The samples were heated to 450°C and cooled to 150°C in zero-grade air (ZGA, dry purified mixture of 80% N_2 and 20% O_2). This step was repeated three times before starting film characterization in order to clear the samples of remanent water vapor.
- The samples were heated to 450°C and cooled to 150°C in 2,000 ppm carbon monoxide diluted in ZGA.
- The samples were heated to 450°C and cooled to 150°C in ZGA.
- The last two steps were repeated four times but with test gas compositions of 10,000 ppm methane, 20,000 ppm propane, 20,000 ppm n-butane and 26 ppm ethanol in ZGA, instead of CO.
- The samples were subjected to 50 thermal cycles (heating to 450°C followed by cooling to 150°C), in the presence of ambient air.
- The samples were tested again using all target gases, repeating the aforementioned procedure. In this way a second set of sample responses was recorded, after 50 aging cycles.
- With the aforementioned procedure, the response of the samples to test gases was recorded after 100, 150 and 250 subsequent aging cycles. In this way five sets of sample responses were recorded.

During the aforementioned measuring cycles, the resistance of the samples was recorded at 5°C intervals as the samples were cooled from 450°C to 150°C; in this way 61

resistance values were recorded for the response of each sensor to each test gas. The cooling rate was 10°C/min. This rate ensures that no significant transient effects are recorded[6] at temperatures above 250°C.

3. Experimental Results and Discussion

Figures 1 and 2 show the logarithm of the conductance of the undoped tin oxide film against the reciprocal temperature (1,000/T) in the presence of ZGA (open circles), of 2,000 ppm carbon monoxide diluted in ZGA (open squares), of 10,000 ppm methane (open triangles), of 20,000 ppm propane (solid circles), of 20,000 ppm n-butane (open hexagons) and of 26 ppm ethanol (open diamonds). The measurements shown in Fig. 1 were taken after the sample had been subjected to 150 temperature cycles, while the measurements shown in Fig. 2 were taken after the sample had been subjected to 250 temperature cycles, according to the analysis in the previous section. In an analogous sense, Figs. 3 and 4 show the response of a tin oxide sensor with palladium additive (deposition time 20 s, SnO_x + Pd3) after it had been subjected to 150 and 250 temperature cycles, respectively. Figures 5 and 6 show the response of a tin oxide sensor with platinum additive (deposition time 30 s, SnO_x + Pt3) after it had been subjected to 150 and 250 temperature cycles, respectively. Figures 7 through 10 show the analogous measurements for indium oxide based sensors (InO_x + Pd3 and InO_x + Pt3) after they had been subjected to 100 and 150 temperature

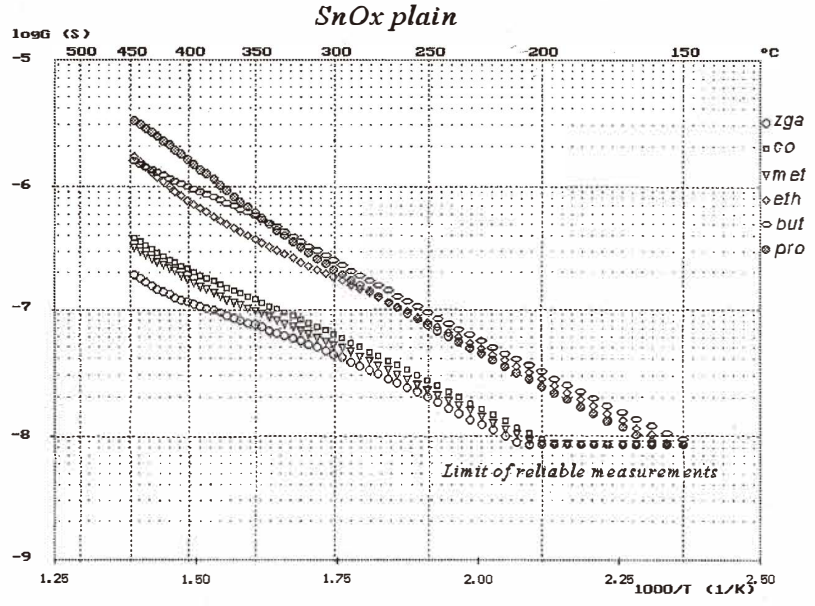

Fig. 1. Log conductance versus reciprocal temperature plot of the plain SnO_x sensor response in the presence of the test gases, after it had been subjected to 150 thermal cycles.

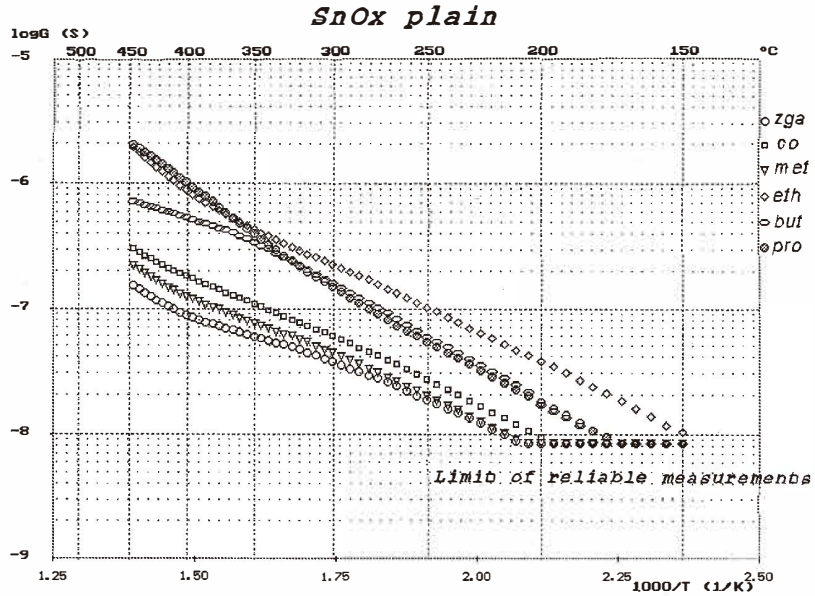

Fig. 2. Log conductance versus reciprocal temperature plot of the plain SnO_x sensor response in the presence of the test gases, after it had been subjected to 250 thermal cycles.

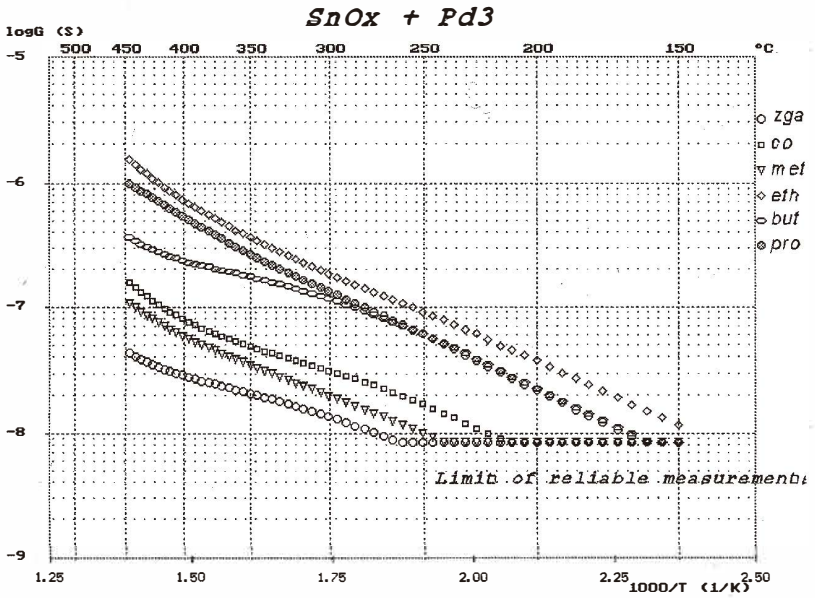

Fig. 3. Log conductance versus reciprocal temperature plot of the SnO_x + Pd3 sensor response in the presence of the test gases, after it had been subjected to 150 thermal cycles.

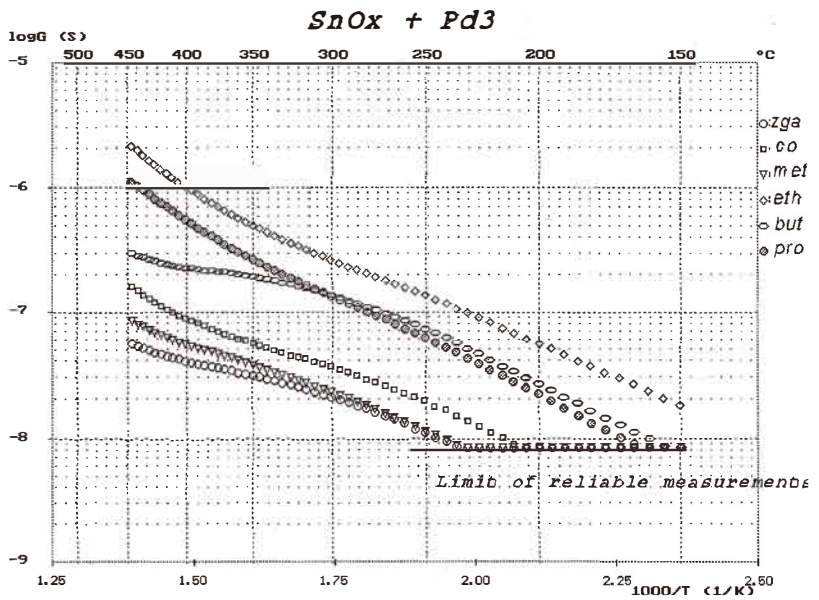

Fig. 4. Log conductance versus reciprocal temperature plot of the SnO_x + Pd3 sensor response in the presence of the test gases, after it had been subjected to 250 thermal cycles.

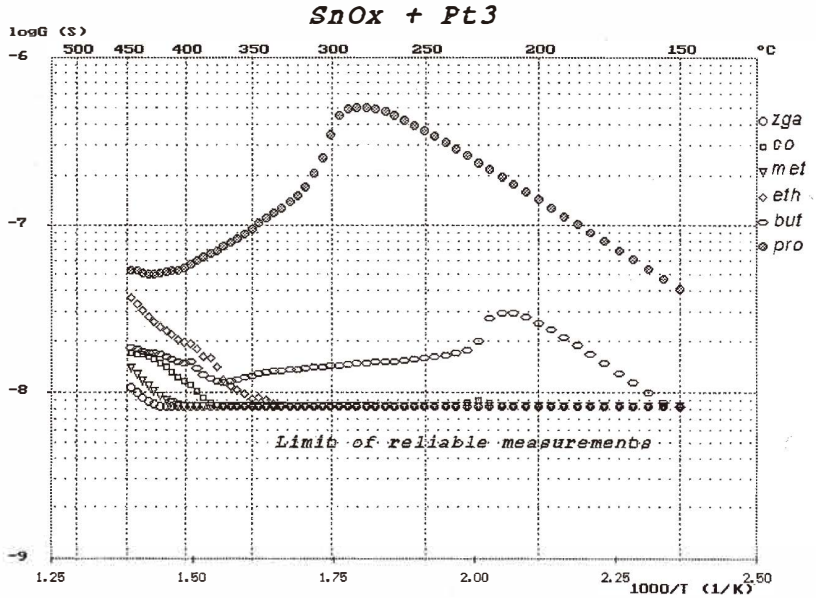

Fig. 5. Log conductance versus reciprocal temperature plot of the SnO_x + Pt3 sensor response in the presence of the test gases, after it had been subjected to 150 thermal cycles.

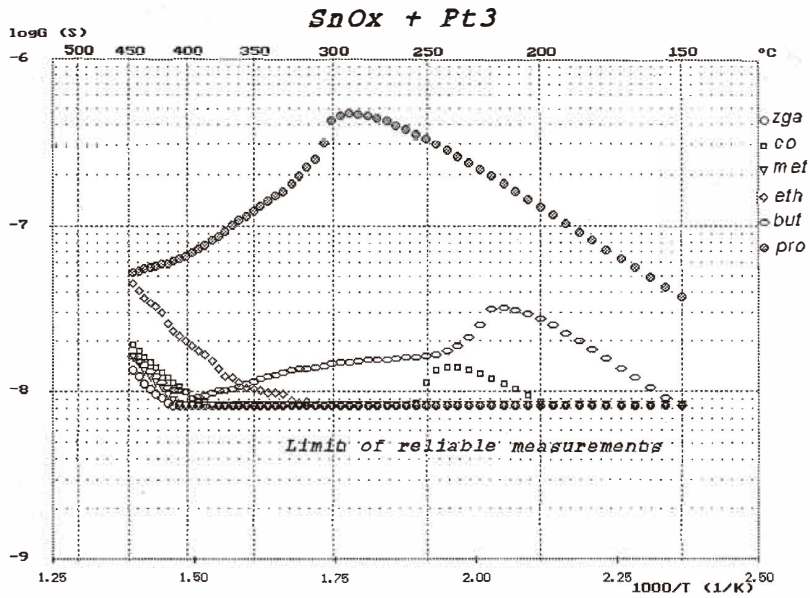

Fig. 6. Log conductance versus reciprocal temperature plot of the SnO_x + Pt3 sensor response in the presence of the test gases, after it had been subjected to 250 thermal cycles.

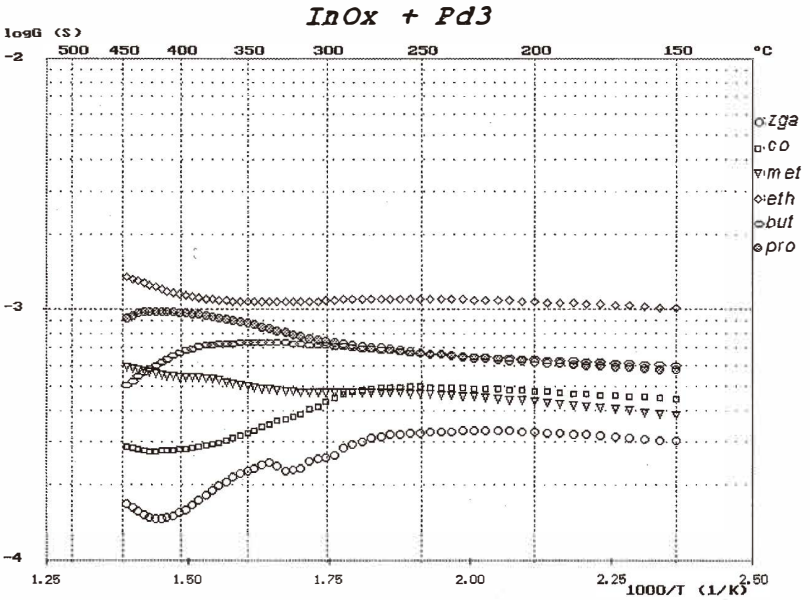

Fig. 7. Log conductance versus reciprocal temperature plot of the InO_x + Pd3 sensor response in the presence of the test gases, after it had been subjected to 100 thermal cycles.

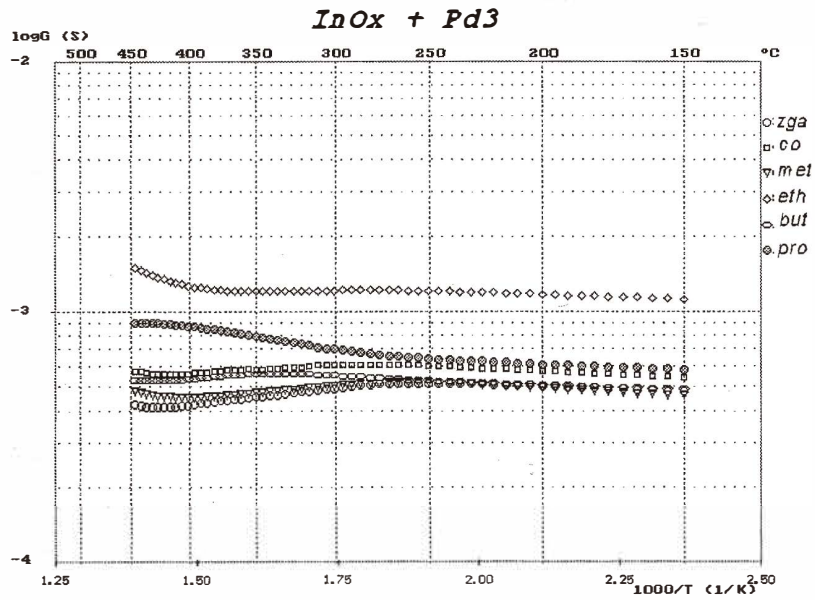

Fig. 8. Log conductance versus reciprocal temperature plot of the InO_x + Pd3 sensor response in the presence of the test gases, after it had been subjected to 150 thermal cycles.

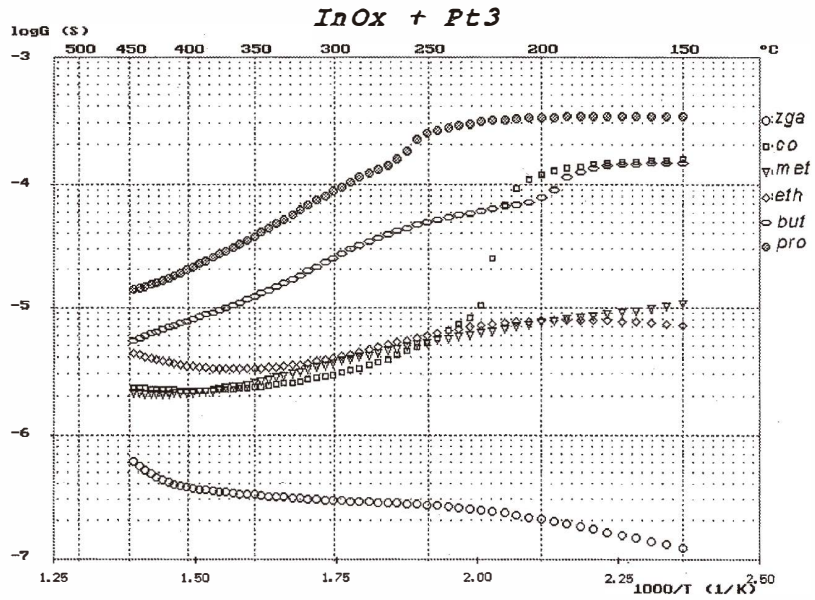

Fig. 9. Log conductance versus reciprocal temperature plot of the InO_x + Pt3 sensor response in the presence of the test gases, after it had been subjected to 100 thermal cycles.

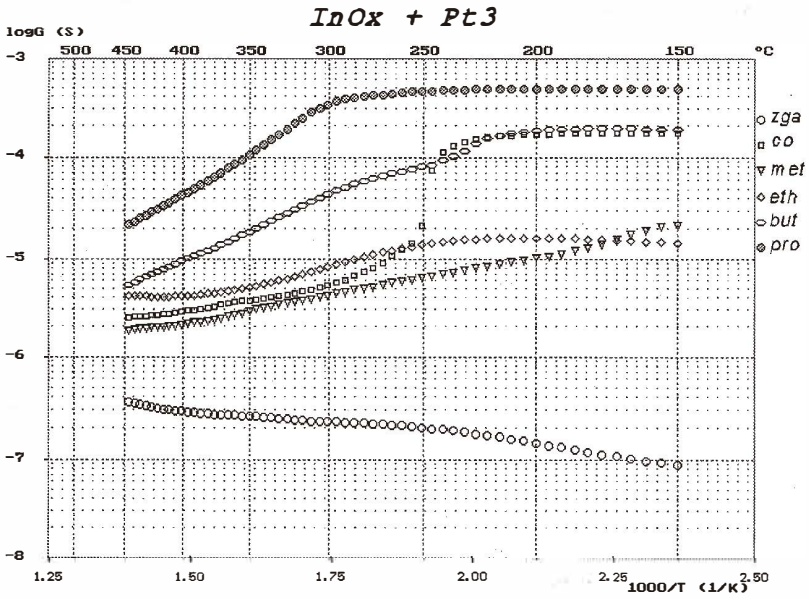

Fig. 10. Log conductance versus reciprocal temperature plot of the InO_x + Pt3 sensor response in the presence of the test gases, after it had been subjected to 150 thermal cycles.

cycles. The response of the indium oxide sensor without additive is not presented because the sensor did not respond to the test gases after thermal treatment. Strong degradation of this sensor was observed after only a few temperature cycles. In addition, plain indium oxide sensors have not shown an interesting response even the first time that they had been exposed to the test gases.

3.1 *Statistical treatment of experimental results*

The acquired experimental data include resistance values for both tin and indium oxide based sensors, covering a range of 2–4 orders of magnitude (indium oxide based sensors are far more conductive than tin oxide based ones; platinum-doped tin oxide sensors in particular exhibit nonmeasurable conductance values). As a consequence, a scaling technique is necessary in order to compensate for the large conductance variances. A simple preprocessing technique that gives each variable equal weighting by adjusting the original data to remove inadvertent weighting on values covering a wide range was adopted and is briefly described below.

Vectors were used to represent the response of the sensors. Two different vector definitions were used: one for the characterization of sensor selectivity properties and the other for the characterization of sensor stability or interdependence properties. In order to characterize the selectivity of a sensor, five vectors representing the response of the sensor to each of the five test gases were created from the measurement data. Each vector includes the resistance values of the sensor in the presence of the corresponding test gas in the

temperature region from 150 to 450°C, recorded at 5°C intervals; thus the size of each vector is 61 ((450 – 150)/5 + 1). In order to characterize the stability of a sensor or the interdependence of two sensors, the aforementioned five vectors were concatenated into one vector of size 5×61. The first 61 elements of this concatenated vector include the resistance values of the sensor obtained in the presence of CO, the next 61 elements include the resistance values in the presence of methane, and so on. The sequence of concatenation does not influence the results of the calculations performed and can be chosen arbitrarily, as long as it is the same for all sensors. This will become obvious from the mathematical treatment that follows.

The original data have been autoscaled so that the vector elements of each sensor are mean centered with a standard deviation of one. The following relationship is used for the calculation of the autoscaled data: [1]

$$r_i' = \frac{r_i - r_{av}}{\sigma}, \quad i = 1..N, \tag{1}$$

where r_{av} is the average resistance over all vector elements of the current sensor and σ is the standard deviation of the sample according to the following formula:[1]

$$\sigma^2 = \frac{\sum_{i=1}^{N} (r_i - r_{av})^2}{N - 1}, \tag{2}$$

where N equals the size of the vector. If the vector contains data acquired in the presence of only one test gas (selectivity characterization), then $N = 61$. In the case of the vectors that contain data for all test gases (stability and interdependence characterization), $N = 5 \times 61$.

A measure of the similarity of two vectors is given by their correlation, which equals the covariance of the autoscaled data, according to the following relationships:[1]

$$\rho_{xy} = \frac{1}{N-1} \cdot \sum_{i=1}^{N} \frac{x_i - x_{av}}{\sigma_x} \cdot \frac{y_i - y_{av}}{\sigma_y} = \sigma_{xy}^2 = \frac{1}{N-1} \cdot \sum_{i=1}^{N} x_i' \cdot y_i'. \tag{3}$$

Here x_i' and y_i' are the autoscaled data of the two response vectors $\boldsymbol{x}$ and $\boldsymbol{y}$. Using the aforementioned mathematical treatment we can determine the stability and selectivity of a sensor or the interdependence of two sensors with a correlation coefficient. More specifically, we can:

- Quantify the stability of a sensor, if $\boldsymbol{x}$ is the response vector of a sensor to all test gases before the aging procedure and $\boldsymbol{y}$ is the response vector of the same sensor to the same test gases after the aging procedure. If the correlation coefficient has a value close to unity the sensor can be characterized as stable, while if it has a value close to zero it can be characterized as unstable.

- Quantify the interdependence of two sensors in response to all test gases, if $\boldsymbol{x}$ is the response vector of one sensor and $\boldsymbol{y}$ is the response vector of a second sensor. The correlation coefficient of the autoscaled vectors of two sensors should be close to unity if their responses are linearly associated and close to zero if their responses are markedly different.
- Quantify the selectivity of a sensor to different test gases, if $\boldsymbol{x}$ is the response vector of a sensor to a specific test gas and $\boldsymbol{y}$ is the response vector of the same sensor to a different test gas. If the correlation coefficient is close to unity then the sensor cannot distinguish between the presence of these two gases.

3.2 *Sensor stability results*

The effect of aging on sensor response is obvious from Figs. 1 through 10. A drift in the conductance against temperature curves with continuous thermal treatment can easily be observed.

Table 1 shows the correlation coefficients which characterize the stability of our sensors, evaluated according to the procedure described in the previous section. Values close to unity (> 0.9) indicate minimal degradation, while values close to zero indicate major change in the sensor's electrical characteristics.

The first column of Table 1 indicates that the first thermal treatment that a sensor is subjected to after fabrication has a major influence on its response. Recall that none of the sensors tested have been annealed. It is a common practice to subject sensors to an

Table 1
Coefficients correlating the responses of the sensors before and after thermal treatment.

	Effect of aging				
	1st vs after 50 cycles	after 50 vs after 100	after 100 vs after 150	after 150 vs after 250	after 50 vs after 250
SnO_x plain	0.908	0.981	0.991	0.968	0.898
SnO_x + Pd1	0.545	0.975	0.983	0.928	0.811
SnO_x + Pd2	0.668	0.861	0.997	0.985	0.836
SnO_x + Pd3	0.483	0.775	0.997	0.994	0.790
SnO_x + Pt1	0.589	0.954	0.853	0.976	0.862
SnO_x + Pt2	0.346	0.836	0.969	0.938	0.676
SnO_x + Pt3	0.891	0.855	0.946	0.975	0.848
SnO_x + Pt4	0.785	0.868	0.975	0.986	0.854
InO_x + Pd1	0.880	0.619	0.239	0.837	0.811
InO_x + Pd2	0.191	0.120	0.046	0.023	0.045
InO_x + Pd3	0.875	0.810	0.639	0.769	0.162
InO_x + Pd4	0.848	0.836	0.660	0.171	0.014
InO_x + Pt1	−0.166	0.666	0.798	0.645	−0.100
InO_x + Pt2	−0.164	−0.257	0.896	0.951	−0.133
InO_x + Pt3	−0.124	0.248	0.945	0.896	−0.119
InO_x + Pt4	0.083	0.765	0.967	0.914	0.587

annealing period of some hours or days at temperatures slightly higher than their operating temperature, in order to stabilize them. Annealing causes structural changes in oxygen-deficient metal oxides, such as tin and indium oxide films,[7,8] exerting a profound influence on their electrical properties. In addition, the structure of noble metal clusters (Pd and Pt) on the surface of semiconducting oxides is modified by thermal treatment. Recall that electron beam evaporation was carried out at ambient temperature. It is known[9] that when thin discontinuous metal films are subjected to high temperatures, small metal islands aggregate and form particles with large average dimensions. It is obvious (Table 1) that the undoped film is more stable than the doped ones, and this property may be attributed to the transformations occurring on the catalyst structure of the surface-doped sensors.

Further investigation of Table 1 reveals that tin oxide based sensors are more stable than indium oxide based ones. This is due to the sharp conductance peaks at certain temperature regions which are observed for indium oxide based films. The small correlation coefficient values observed for InO_x sensors can be attributed to the fact that the temperature of the maximum conductivity decreases after successive thermal cycles.

3.3 *Interdependence of sensors*

The response of each tin oxide sensor is correlated with the response of all other tin oxide sensors following the same thermal treatment, as shown in Table 2. The response of each indium oxide sensor is correlated with the response of all other indium oxide sensors following the same thermal treatment, as shown in Table 3. The first rows for each sensor of Tables 2 and 3 show the correlation coefficients for the first measuring procedure (without thermal pretreatment), to which the sensors were subjected, the second rows show the correlation coefficients corresponding to the response of the sensors after 50 thermal cycles, and so on. The values in Tables 2 and 3 which are greater than 0.9, implying strong interdependence of sensors, are underlined.

The undoped tin oxide sensor and the tin oxide sensors doped with palladium (specifically the two tin oxide sensors with thick palladium layers, SnO_x + Pd2 and SnO_x + Pd3) seem to be strongly correlated, while the tin oxide sensor with the thin palladium layer (SnO_x + Pd1) shows a response different from those of the other two palladium-doped tin oxide sensors. The interdependence of the palladium-doped sensors becomes obvious after some thermal treatment, which is believed to cause significant changes in both the oxygen deficiency of the tin oxide and the structure of the catalytic layer. In a pattern recognition multisensor array, only one of the plain and the two correlated palladium-doped sensors would be needed, while the incorporation of a second sensor would be superfluous.

An interesting interdependence is observed in the response of the two tin oxide sensors with the thick platinum layers, SnO_x + Pt3 and SnO_x + Pt4 (correlation coefficient of 0.89). The behavior of tin oxide films doped with thick layers of an additive is very similar, implying a saturation effect related to the thickness of the additive.

Concerning indium oxide based sensors, a strong interdependence of all palladium-doped InO_x sensors is observed, mainly in their response after 50 thermal cycles. Since from Table 1 it can be seen that palladium-doped indium oxide sensors are unstable, we can assume that the sensors lose their sensing properties after intense thermal treatment.

Table 2
Correlation coefficients showing the interdependence of tin oxide sensors after thermal treatment. The first row for each sensor shows the coefficients corresponding to the responses of the sensors without thermal treatment, the second row corresponds to the responses of the sensors after 50 thermal cycles, etc.

	Interdependenne of tin oxide based sensors							
	SnO_x plain	SnO_x + Pd1	SnO_x + Pd2	SnO_x + Pd3	SnO_x + Pt1	SnO_x + Pt2	SnO_x + Pt3	SnO_x + Pt4
SnO_x plain	1	0.81	0.64	0.34	0.36	0.49	0.46	0.44
	1	0.43	0.86	0.82	0.32	0.15	0.45	0.27
	1	0.49	0.92	0.92	0.36	0.22	0.28	0.30
	1	0.57	0.93	0.94	0.41	0.26	0.31	0.29
	1	0.68	0.86	0.95	0.39	0.33	0.19	0.18
SnO_x + Pd1	*	1	0.58	0.14	0.11	0.47	0.21	0.17
		1	0.40	0.38	0.12	0.42	0.49	0.26
		1	0.53	0.60	0.18	0.49	0.38	0.31
		1	0.57	0.66	0.16	0.48	0.31	0.27
		1	0.65	0.72	0.27	0.52	0.29	0.34
SnO_x + Pd2	*	*	1	0.77	0.34	0.57	0.28	0.33
			1	0.97	0.30	0.15	0.43	0.38
			1	0.98	0.36	0.24	0.31	0.34
			1	0.97	0.40	0.26	0.36	0.36
			1	0.96	0.43	0.32	0.37	0.40
SnO_x + Pd3	*	*	*	1	0.49	0.50	0.33	0.40
				1	0.33	0.17	0.40	0.43
				1	0.42	0.28	0.37	0.41
				1	0.42	0.30	0.38	0.36
				1	0.41	0.35	0.30	0.31
SnO_x + Pt1	*	*	*	*	1	0.84	0.89	0.78
					1	0.51	0.53	0.54
					1	0.68	0.57	0.69
					1	0.60	0.50	0.56
					1	0.70	0.55	0.63
SnO_x + Pt2	*	*	*	*	*	1	0.80	0.71
						1	0.28	0.27
						1	0.50	0.47
						1	0.49	0.49
						1	0.53	0.58
SnO_x + Pt3	*	*	*	*	*	*	1	0.87
							1	0.79
							1	0.88
							1	0.89
							1	0.89
SnO_x + Pt4	*	*	*	*	*	*	*	1
								1
								1
								1
								1

Table 3
Correlation coefficients showing the interdependence of indium oxide sensors after thermal treatment. The first row for each sensor shows the coefficients corresponding to the responses of the sensors without thermal treatment, the second row corresponds to the responses of the sensors after 50 thermal cycles, etc.

	Interdependence of indium oxide based sensors							
	InO_x + Pd1	InO_x + Pd2	InO_x + Pd3	InO_x + Pd4	InO_x + Pt1	InO_x + Pt2	InO_x + Pt3	InO_x +Pt4
InO_x	1	0.20	0.74	0.77	0.46	0.55	0.41	0.47
+ Pd1	1	0.93	0.93	0.95	−0.19	−0.09	−0.16	0.34
	1	0.09	0.74	0.71	−0.20	0.15	−0.01	0.02
	1	0.87	0.57	0.79	0.58	0.41	0.83	0.81
	1	−0.05	0.35	0.17	0.57	0.29	0.74	0.71
InO_x	*	1	0.29	0.29	−0.03	0.02	−0.04	−0.03
+ Pd2		1	0.99	0.99	−0.41	−0.12	−0.37	0.28
		1	0.16	0.19	0.10	0.11	0.20	0.19
		1	0.74	0.85	0.32	0.43	0.60	0.59
		1	0.12	0.03	0	−0.08	−0.05	−0.07
InO_x	*	*	1	1.0	0.01	0.16	−0.05	0.01
+Pd3			1	0.99	−0.32	−0.15	−0.28	0.35
			1	0.96	0.03	0.60	0.44	0.50
			1	0.92	−0.21	0.49	0.21	0.19
			1	0.62	−0.11	0.42	0.02	0.01
InO_x	*	*	*	1	0.06	0.20	−0.01	0.05
+ Pd4				1	−0.35	−0.13	−0.32	0.29
				1	0.12	0.57	0.50	0.52
				1	0.09	0.62	0.52	0.50
				1	−0.13	0.10	−0.12	−0.14
InO_x	*	*	*	*	1	0.96	0.96	0.98
+ Pt1					1	−0.19	0.98	0.50
					1	0.32	0.79	0.63
					1	0.03	0.84	0.86
					1	0.04	0.77	0.73
InO_x	*	*	*	*	*	1	0.86	0.93
+ Pt2						1	−0.23	−0.42
						1	0.65	0.73
						1	0.39	0.43
						1	0.41	0.47
InO_x	*	*	*	*	*	*	1	0.98
+ Pt3							1	0.61
							1	0.95
							1	0.99
							1	0.99
InO_x	*	*	*	*	*	*	*	1
+ Pt4								1
								1
								1
								1

However, it is interesting to note that the two InO_x sensors with the thick palladium layers (InO_x + Pd3 and InO_x + Pd4) exhibit very close correlation coefficients, supporting the assumption that a saturation effect is related to the thickness of the additive layer.

Finally, interdependence is also observed for the four platinum-doped indium oxide sensors, as derived from the correlation coefficients in Table 3. In this case, strong interdependence is observed before the sensors are subjected to any thermal treatment. However, the two sensors with the thick platinum layers remain strongly interdependent even after 250 thermal cycles.

It is worth noting that all sensors with different sensing layers (tin or indium oxide) or with different types of doping (palladium or platinum) seem to be totally independent of each other. Sensors with the same sensing layer and the same additive exhibit similar responses. Moreover, the degree of their interdependence seems to be conserved despite the increasing number of thermal cycles to which the sensors were subjected. The above information may be useful for the selection of sensors to be incorporated in a multisensor pattern recognition array, without taking into account the actual pattern recognition method used.

3.4 *Sensor selectivity*

In order to quantify the selectivity of our sensors for the five gases tested, coefficients were calculated to correlate the response of a sensor to a test gas after a thermal treatment with the response of the same sensor to all other test gases after the same thermal treatment. This procedure was repeated for all sixteen sensors tested and for all of the aging periods to which the sensors were subjected. For clarity, only coefficients correlating the response of selected sensors after 100 thermal cycles are presented in Tables 4 through 9.

Table 4 shows coefficients correlating the response of the plain tin oxide sensor to all test gases. Since all correlation coefficients are very close to unity (>0.9) it is obvious that the plain SnO_x sensor is not selective. Correlation coefficients very close to unity were also found for the response of this sensor without thermal treatment, after 50 thermal cycles, after 150 thermal cycles and after 250 thermal cycles. Recall that the data presented in Table 4 are irrelevant to sensor sensitivity. This sensor is very sensitive to most of the gases tested, especially ethanol, but the temperature dependence of the sensor response to different test gases is very similar. Sensitivity values corresponding to different gases may be very different, as is obvious from Figs. 1 and 2. It is also evident from Figs. 1 and 2 that the sensor is not selective, since sensor conductance as a function of temperature is very similar for all test gases.

Table 5 shows the correlation coefficients for a palladium-doped tin oxide sensor subjected to 100 thermal cycles, with the palladium of intermediate thickness (SnO_x + Pd2). Similar values were obtained for the tin oxide sensors with thin and thick palladium layers (SnO_x + Pd1 and SnO_x + Pd3). Table 5 shows that the palladium-doped tin oxide sensors are not selective, especially for ethanol, butane and propane, as it is also obvious from Figs. 3 and 4.

Table 6 shows correlation coefficient values of the platinum-doped tin oxide sensor, with a platinum evaporation time of 30 s (SnO_x + Pt3), after it had been subjected to 100 thermal cycles. The response of the same sensor after 150 and 250 thermal cycles is shown

Table 4
Correlation coefficients for the selectivity of the plain SnO_x sensor after 100 thermal cycles.

	Selectivity of plain SnO_x sensor after 100 thermal cycles				
	CO	CH_4	C_2H_5OH	C_4H_{10}	C_3H_8
CO	1.0000	0.9964	0.9320	0.9242	0.9238
CH_4	*	1.0000	0.9099	0.9023	0.9015
C_2H_5OH	*	*	1.0000	0.9977	0.9990
C_4H_{10}	*	*	*	1.0000	0.9996
C_3H_8	*	*	*	*	1.0000

Table 5
Correlation coefficients for the selectivity of the SnO_x + Pd2 sensor after 100 thermal cycles.

	Selectivity of SnO_x + Pd2 sensor after 100 thermal cycles				
	CO	CH_4	C_2H_5OH	C_4H_{10}	C_3H_8
CO	1.0000	0.9290	0.9271	0.9089	0.9126
CH_4	*	1.0000	0.8102	0.7752	0.7847
C_2H_5OH	*	*	1.0000	0.9980	0.9989
C_4H_{10}	*	*	*	1.0000	0.9998
C_3H_8	*	*	*	*	1.0000

Table 6
Correlation coefficients for the selectivity of the SnO_x + Pt3 sensor after 100 thermal cycles.

	Selectivity of SnO_x + Pt3 sensor after 100 thermal cycles				
	CO	CH_4	C_2H_5OH	C_4H_{10}	C_3H_8
CO	1.0000	0.9369	0.7783	0.4335	−0.6718
CH_4	*	1.0000	0.6189	0.4536	−0.5155
C_2H_5OH	*	*	1.0000	0.2957	−0.8129
C_4H_{10}	*	*	*	1.0000	−0.1737
C_3H_8	*	*	*	*	1.0000

Table 7
Correlation coefficients for the selectivity of the InO_x + Pd3 sensor after 100 thermal cycles.

	Selectivity of InO_x + Pd3 sensor after 100 thermal cycles				
	CO	CH_4	C_2H_5OH	C_4H_{10}	C_3H_8
CO	1.0000	−0.8369	−0.6421	0.1724	−0.9113
CH_4	*	1.0000	0.8154	−0.1118	0.9454
C_2H_5OH	*	*	1.0000	−0.6345	0.6415
C_4H_{10}	*	*	*	1.0000	0.0735
C_3H_8	*	*	*	*	1.0000

Table 8
Correlation coefficients for the selectivity of the InO_x + Pd3 sensor after 250 thermal cycles.

	Selectivity of InO_x + Pd3 sensor after 250 thermal cycles				
	CO	CH_4	C_2H_5OH	C_4H_{10}	C_3H_8
CO	1.0000	0.9327	0.9120	0.9380	0.9319
CH_4	*	1.0000	0.8192	0.9087	0.9104
C_2H_5OH	*	*	1.0000	0.8222	0.8099
C_4H_{10}	*	*	*	1.0000	0.9836
C_3H_8	*	*	*	*	1.0000

Table 9
Correlation coefficients for the selectivity of the InO_x + Pt1 sensor after 100 thermal cycles.

	Selectivity of InO_x + Pt1 sensor after 100 thermal cycles				
	CO	CH_4	C_2H_5OH	C_4H_{10}	C_3H_8
CO	1.0000	0.9608	0.1575	0.8992	0.8112
CH_4	*	1.0000	−0.0105	0.9522	0.8874
C_2H_5OH	*	*	1.0000	−0.2583	−0.4180
C_4H_{10}	*	*	*	1.0000	0.9761
C_3H_8	*	*	*	*	1.0000

in Figs. 5 and 6, respectively. The correlation coefficients of Table 6 indicate that this sensor is markedly selective (values less than 0.9), especially in the case of butane and propane. The relatively high correlation coefficient values for carbon monoxide, ethanol and methane can be attributed to the fact that the resistance of the sensor in the presence of these gases exhibits nonmeasurable values. An analogous behavior was observed for all platinum-doped sensors, independent of the thermal cycles to which they were subjected. We can conclude that selectivity to butane and propane which is obvious from Figs. 5 and 6 can be described quantitatively using the correlation coefficient values of Table 6.

The response of the palladium-doped indium oxide sensor with an evaporation time of 20 s (InO_x + Pd3), after it had been subjected to 100 thermal cycles is shown in Fig. 7. The correlation coefficients calculated using the data presented in Fig. 7 are shown in Table 7, while the correlation coefficients of the same sensor after it was submitted to 250 thermal cycles are shown in Table 8. It is obvious that this sensor is not selective, exhibiting a strong interdependence concerning its response to all test gases.

Table 9 shows the correlation coefficients calculated for the response of an indium oxide sensor doped with platinum (platinum evaporation time of 10 s, InO_x + Pt1). From the data in Table 9 this sensor seems to be selective to ethanol. The response of the platinum-doped indium oxide sensors exhibits a conductance step at a temperature of around 200 – 300°C in the presence of carbon monoxide, butane and propane. This step is shown in Figs. 9 and 10, and is more distinct in the case of carbon monoxide. However, since this step is not very sharp (as in the case of platinum-doped tin oxide sensors), Table 9 does not clearly show a selective sensor. Analogous results were derived for all other platinum-doped indium oxide sensors. The main advantage of indium oxide based sensors is their high conductivity, which is 2–4 orders of magnitude higher than that of tin oxide based sensors.

4. Conclusions

Sixteen metal (tin and indium) oxide semiconducting thin films with different noble metals (palladium and platinum) deposited onto their surfaces as catalysts were considered as sensors for various reducing or combustible gases. Efforts have been focused on sensor characterization concerning temperature stability, interdependence and selectivity. A

simple nonparametric technique (i.e., correlation coefficient evaluation) has been chosen from a variety of proposed statistical methods[10,11,12] for gas sensing applications. Although the method used is very simple, it can extract useful information from our data. The most interesting results are summarized as follows:

- The marked resistance variations observed during the first thermal treatment of a nonannealed sensor are due to both structural changes in the oxygen-deficient metal oxide film and the transformations in the structure of the additive layer.
- Tin oxide based sensors are generally more stable than indium oxide based ones (Table 1).
- An undoped tin oxide sensor is more stable than doped tin oxide sensors (Table 1). This may be attributed to the additional degradation of the catalytic layer.
- The same metal oxide films with different additives exhibit noncorrelated responses (Tables 2 and 3).
- The same metal oxide films with different thicknesses of the same additive are interdependent. This interdependence is lost in some sensors after thermal treatment, due to sensor degradation (Tables 2 and 3).
- Sensors with relatively thick additive layers remain strongly interdependent after severe thermal treatment (Tables 2 and 3).
- Undoped or palladium-doped sensors show poor selectivity (Tables 4, 5, 7 and 8).
- Platinum-doped sensors (SnO_x- and InO_x-based) exhibit marked selectivity (Tables 6 and 9). The main disadvantage of platinum-doped SnO_x sensors, which exhibit both selectivity and stability, is their relatively low conductivity (Figs 5 and 6), which renders them unsuitable for practical applications. On the other hand, platinum-doped InO_x sensors exhibit satisfactory stability and selectivity, and also exhibit sufficient conductivity, which makes them suitable for practical applications. An alternative statistical method may be more appropriate for the successful interpretation of data related to the response of InO_x sensors, in order to compensate for the temperature shift of their response with continuous thermal treatment.

References

1 P . T. Moseley, J. O. W. Norris and D. E. Williams: Techniques and Mechanisms in Gas Sensing (Adam Hilger, Bristol, 1991) chapter 14, pp. 347-384.
2 J. W. Gardner, H. V. Shurmer and T. T. Tan: Sensors and Actuators **B6** (1992) 71.
3 V. Lantto, P. Romppainen and S. Leppavuori: Sensors and Actuators **14** (1988) 149.
4 C. D. Tsiogas and J. N. Avaritsiotis: Vacuum **45** (12) (1994) 1181.
5 C. A. Papadopoulos and J. N. Avaritsiotis: Sensors and Actuators **B28** (3) (1996) 201.
6 P. D. Skafidas, D. S. Vlachos and J. N. Avaritsiotis: Sensors and Actuators **B21** (1994) 109.
7 S. V. Kolluri and A. N. Chandorkar: Thin Solid Films **230** (1993) 39.
8 D. F. Cox, T. B. Fryberger and S. Semancik: Surface Science **224** (1989) 121.
9 C. A. Neugebauer and M. B. Webb: Journal of Applied Physics **33** (1) (1962) 74.
10 M. S. Nayak, R. Dwivedi and S. K. Srivatsava: Sensors and Actuators **B12** (1993) 103.
11 H. Odeberg: Sensors and Actuators **A36** (1993) 89.
12 W. P. Carey and S. S. Yee: Sensors and Actuators **B9** (1992) 113.